One-Pot Synthesis of Single-Source Precursors for Nanocrystalline LED Phosphors $M_2Si_5N_8:Eu^{2+}$ (M = Sr, Ba)

Martin Zeuner,[†] Peter J. Schmidt,[‡] and Wolfgang Schnick*,[†]

Department Chemie und Biochemie, Ludwig-Maximilians-Universität München, Butenandtstrasse 5-13 (D), D-81377 München, Germany, and Philips Research Europe Aachen, Weisshausstrasse 2, D-52066 Aachen, Germany

Received February 5, 2009. Revised Manuscript Received April 9, 2009

Highly efficient red-emitting nitridosilicate phosphors $Sr_2Si_5N_8:Eu^{2+}$ and $Ba_{1.5}Sr_{0.5}Si_5N_8:Eu^{2+}$ (doping level 1 %) applicable to phosphor converted pc-LEDs were synthesized in nanocrystalline form at low temperatures employing a novel single-source precursor approach. Synthesis starts from nanocrystalline silicon and uses mixed metal amides $M(NH_2)_2$ with M = Sr, Ba, Eu as reactive intermediates. In a second approach, a single-source precursor mixture obtained from a one-pot reaction of the corresponding elements (Sr/Ba, Eu, Si) was obtained in supercritical ammonia. Thermoanalytical in situ investigations gain a deeper insight into the degradation mechanism of the mixed metal amide precursors and revealed the onset for the formation of the 2-5-8 phosphor materials at temperatures slightly above 900 °C. Formation of the products is complete below 1400 °C. Under these conditions, the nitridosilicate phosphors form spherically shaped particles with crystallites of 200 nm in size. Spherical particles are desirable for phosphor application because light extraction may be improved by decreased light trapping and re-absorption losses. As a major advantage of the one-pot precursor approach, the exact Sr/Ba content in the solid solution series $Sr_{2-x}Ba_xSi_2N_8:Eu^{2+}$ and the doping concentration of Eu^{2+} can easily be controlled in a wide range by the relative amount of the elemental starting materials (Sr, Ba, Eu, Si). Simultaneously, thorough mixing of these elements down to an atomic level (Sr, Ba, Eu) or at least at nanoscopic dimensions (silicon) is achieved by the solution approach. As a consequence, no milling and pre-reaction steps are necessary which might give rise to contamination. Advantageously, this approach can easily be extended to large-scale processes by simultaneously preserving complete mixing. Furthermore, the influence of the starting materials (single-source precursor, nanocrystalline silicon) and the reaction conditions on the crystal shape and finally on the luminescence properties of the products was investigated. The obtained nanophosphors exhibit luminescence properties comparable to coarsely crystalline nitridosilicate phosphor powders prepared by conventional high-temperature processing.

Introduction

Upon doping with lanthanide ions (e.g. Eu^{2+}, Ce^{3+}), a number of nitridosilicates and oxonitridosilicates emerged as highly efficient luminescent materials (phosphors) that found considerable industrial application in white light-emitting diodes (LEDs).[1−7] Excitation with near-UV or blue light causes these Eu^{2+}-phosphors to emit visible light due to the 4f−5d parity-allowed optical transition of Eu^{2+}, which is sensitive to the crystal field and covalency of a given host lattice site. The Eu^{2+} excitation and emission bands of nitridic hosts are significantly red shifted, compared to oxidic compounds, because of the covalent bonding interactions between Eu^{2+} and the N ligands (nephelauxetic effect). This allows the Eu^{2+} doped phosphors to be used as down-conversion luminescence materials for white-light LEDs.[6] Eu^{2+}-doped nitridic phosphors show outstanding luminescence properties like good quantum efficiency, radiation stability, and excellent thermal quenching behavior. Additionally, the lanthanide ion Eu^{2+} supplies an emission band shape well suited for 2- and 3-pc (phosphor-converted)-LED applications.[7,8] Prominent examples of such advanced phosphor materials are $CaAlSiN_3:Eu^{2+}$ [9,10] and the solid solution series $Sr_{2-x-y}Ba_xCa_ySi_5N_8:Eu^{2+}$ (so-called 2-5-8 phosphors).[2,6,11]

* To whom correspondence should be addressed. Fax: (49)89-2180-77440. E-mail: wolfgang.schnick@uni-muenchen.de.
† Ludwig-Maximilians-Universität München.
‡ Philips Research Europe Aachen.

(1) Höppe, H. A.; Lutz, H.; Morys, P.; Schnick, W.; Seilmeier, A. *J. Phys. Chem. Solids* **2000**, *61*, 2001.
(2) Mueller-Mach, R.; Mueller, G.; Krames, M. R.; Höppe, H. A.; Stadler, F.; Schnick, W.; Juestel, T.; Schmidt, P. *Phys. Status Solidi A* **2005**, *202*, 1727.
(3) Li, Y. Q.; van Steen, J. E. J.; van Krevel, J. W. H.; Botty, G.; Delsing, A. C. A.; DiSalvo, F. J.; deWith, G.; Hintzen, H. T. *J. Alloys Compd.* **2006**, *417*, 273.
(4) Li, Y. Q.; deWith, G.; Hintzen, H. T. *J. Solid State Chem.* **2008**, *181*, 515.
(5) Piao, X.; Horikawa, T.; Hanzawa, H.; Machida, K. *Appl. Phys. Lett.* **2006**, *88*, 161908.
(6) Xie, R.-J.; Hirosaki, N. *Sci. Technol. Adv. Mater.* **2007**, *8*, 588.
(7) Xie, R.-J.; Hirosaki, N.; Kimura, N.; Sakuma, K.; Mitomo, M. *Appl. Phys. Lett.* **2007**, *90*, 191101/1.
(8) Schmidt, P.; Tuecks, A.; Meyer, J.; Bechtel, H.; Wiechert, D.; Mueller-Mach, R.; Mueller, G.; Schnick, W. *Proc. SPIE* **2007**, *6669*, 66690P/1–66690P/9; Seventh International Conference on Solid State Lighting, 2007.
(9) Uheda, K.; Hirosaki, N.; Yamamoto, Y.; Naito, A.; Nakajima, T.; Yamamoto, H. *Solid State Lett.* **2006**, *9*, H22.
(10) Uheda, K.; Hirosaki, N.; Yamamoto, H. *Phys. Status Solidi A* **2006**, *203*, 2712.
(11) Piao, X.; Machida, K.; Horikawa, T.; Hanzawa, H. *Appl. Phys. Lett.* **2007**, *91*, 041908.

10.1021/cm900341f CCC: $40.75
Published on Web 05/01/2009

Hence, much effort has been directed toward the synthesis of new nitridosilicates as host lattices.[12,13] However, the development of optimized synthetic approaches for the known nitridosilicate phosphor materials has also been a major goal.[14,15]

With common starting materials (e.g. silicon nitride, metals and oxides) high-temperature processes between 1550 and 1650 °C are necessary for synthesis of nitridosilicates.[16−21] By use of alternative methods like carbothermal reduction and nitridation (CRN) of oxides,[5] the synthesis temperature has been lowered to 1400−1500 °C. However, the CRN approach may lead to a considerable amount of carbon within the synthesized products reducing luminescence efficiency of the phosphors.[22] Other methods to lower the reaction temperature have been reported (e.g. employment of a sodium flux) for the synthesis of $MSiN_2$ (M = Ca, Sr, Ba) which could be obtained at 900−1100 °C.[23] However, the use of alkali metal fluxes necessitates usage of closed reaction systems (e.g. tantalum ampules) hampering upscaling of these approaches to large-scale processing.

Ammonothermal approaches at relatively low temperatures (500−700 °C) have successfully been applied for crystal growth of binary nitrides AlN or GaN.[24−26] Contrary, similar low-temperature solution-based synthetic approaches leading to multinary nitridosilicates have scarcely been investigated. Recently, the synthesis of $CaAlSiN_3$ starting from a pre-synthesized CaAlSi alloy has been reported at relatively low temperatures by reaction in supercritical ammonia and subsequent thermal annealing. Optimized yields have only been achieved by addition of $NaNH_2$ as a mineralizer, which results in the formation of fissured particles and barlike crystals.[27] Very recently, we have reported another low temperature synthesis approach to nitridosilicate phosphors and the influence of metal amides on the crystal shape and luminescence properties.[28]

In this work, we present the synthesis of single-source precursors for the efficient phosphor materials $Sr_2Si_5N_8:Eu^{2+}$ and $Ba_{2-x}Sr_xSi_5N_8:Eu^{2+}$ in a one-pot approach in supercritical ammonia. The nitridosilicates are obtained by heating the single-source precursors at relatively low temperatures around 1300−1400 °C. This method allows for an easy control of the product composition and homogeneous distribution of the starting elements including the dopant within the products. Moreover tailor made globular phosphor crystallites with a size of 200 nm are accessible due to the use of nanocrystalline silicon. The influence of the employed silicon source (silicon diimide, silicon powder, and nanocrystalline silicon) on the crystal shape and luminescence properties of the phosphor was investigated.

Experimental Section

Unless otherwise stated, all manipulations were performed with rigorous exclusion of oxygen and moisture in flame-dried glassware connected to a Schlenk line, interfaced to a vacuum line (1×10^{-3} mbar), or in an argon-filled glovebox (Unilab, MBraun, Garching, O_2 <0.1 ppm, H_2O <0.1 ppm). Argon (Messer-Griessheim, 5.0) was purified by passage over columns of silica gel (Merck), molecular sieve (Fluka, 4 Å), KOH (Merck, ≥85 %), P_4O_{10} (Roth, ≥99 %, granulate) and titanium sponge at 700 °C (Johnson Matthey, 99.5 %, grain size ≤0.8 cm).

The general procedure for reactions in supercritical NH_3 is described in the following: The elemental starting materials (strontium and/or barium, Sigma-Aldrich, 99.99 %, pieces; europium, Smart-Elements, 99.9 %, pieces) were introduced into a Parr high-pressure vessel (Type 4740) with a Parr gage block (Type 4316) and connected to a vacuum/inert gas line. A sufficient amount of ammonia (Linde, 5.0) was condensed into the vessel by cooling to −80 °C. The autoclave was closed and slowly warmed up to room temperature and then heated at 10 °C/min to the final reaction temperature. A pressure of 300 bar was maintained during the reaction. After 5 days, the vessel was cooled to room temperature and the pressure was reduced carefully. Excessive ammonia was removed by evacuating the autoclave and subsequent flushing with argon. Finally, the vessel was opened in an argon-filled glovebox. The products were obtained as powders and analyzed by FTIR spectroscopy, EDX and XRD analysis.

Synthesis of $Sr_2Si_5N_8:Eu^{2+}$ and $Ba_{2-x}Sr_xSi_5N_8:Eu^{2+}$: A mixture of the pre-synthesized metal amide precursor and nanocrystalline silicon (Alfa Aesar, average grain size 50 nm); silicon powder (Cerac, 99.999 %) or silicon diimide (synthesized according to the literature)[29] was ground and transferred into a tungsten crucible under an argon atmosphere inside a glovebox. After placing the crucible into the center of a water-cooled quartz reactor of a radio-frequency furnace (type IG 10/200 Hy, frequency: 200 kHz, max. electrical output: 12 kW, Hüttinger, Freiburg)[30] under a N_2 atmosphere, the temperature was raised to 800 °C within 60 min. After 3 h, the temperature was increased to 1400 °C within 1 h and maintained for 24 h. Slow cooling to 800 °C within 12 h and quenching to room temperature in 30 min yielded $Sr_2Si_5N_8:Eu^{2+}$ and $Ba_{1.5}Sr_{0.5}Si_5N_8:Eu^{2+}$, respectively.

One pot synthesis of $Sr_2Si_5N_8:Eu^{2+}$ and $Ba_{2-x}Sr_xSi_5N_8:Eu^{2+}$: A mixture of stoichiometric amounts of the elements (Sr/Ba, Eu, Si) were placed into a Parr high-pressure autoclave and reacted

(12) Bachmann, V.; Ronda, C.; Oeckler, O.; Schnick, W.; Meijerink, A. *Chem. Mater.* **2009**, *21*, 316.
(13) Kechele, J.; Hecht, C.; Oeckler, O.; Schmidt, P.; Schnick, W. Chem. Mater. 2009, *21*, (in press).
(14) Xie, R.-J.; Hirosaki, N.; Suehiro, T.; Xu, F.; Mitomo, M. *Chem. Mater.* **2006**, *18*, 5578.
(15) Piao, X.; Machida, K.; Horikawa, T.; Hanzawa, H.; Shimomura, Y.; Kijima, N. *Chem. Mater.* **2007**, *19*, 4592.
(16) Pilet, G.; Höppe, H. A.; Schnick, W.; Esmaeilzadeh, S. *Solid State Sci.* **2005**, *7*, 391.
(17) Schlieper, T.; Milius, W.; Schnick, W. *Z. Anorg. Allg. Chem.* **1995**, *621*, 1037.
(18) Huppertz, H.; Schnick, W. *Acta Crystallogr., Sect. C: Cryst. Struct. Commun.* **1997**, *53*, 1751.
(19) Schlieper, T.; Milius, W.; Schnick, W. *Z. Anorg. Allg. Chem.* **1995**, *621*, 1380.
(20) Stadler, F.; Oeckler, O.; Höppe, H. A.; Möller, M. H.; Pöttgen, R.; Mosel, B. D.; Schmidt, P.; Duppel, V.; Simon, A.; Schnick, W. *Chem.—Eur. J.* **2006**, *12*, 6984.
(21) Höppe, H. A.; Stadler, F.; Oeckler, O.; Schnick, W. *Angew. Chem.* **2004**, *116*, 5656 Angew. Chem. Int. Ed. **2004**, *43*, 5540.
(22) Qiu, J.-Y.; Tatami, J.; Zhang, C.; Komeya, K.; Meguro, T.; Cheng, Y.-B. *J. Eur. Ceram. Soc.* **2002**, *22*, 2989.
(23) Gál, Z. A.; Mallinson, P. M.; Orchard, H. J.; Clarke, S. J. *Inorg. Chem.* **2004**, *43*, 3998.
(24) Wang, B.; Callahan, M. J. *Cryst. Growth Des.* **2006**, *6*, 1227.
(25) Peters, D. *J. Cryst. Growth* **1990**, *104*, 411.
(26) Hashimoto, T.; Wu, F.; Saito, M.; Fujito, K.; Speck, J. S.; Nakamura, S. *J. Cryst. Growth* **2008**, *310*, 876.
(27) Li, J.; Watanabe, T.; Sakamoto, N.; Wada, H.; Setoyama, T.; Yoshimura, M. *Chem. Mater.* **2008**, *20*, 2095.
(28) Zeuner, M.; Hintze, F.; Schnick, W. *Chem. Mater.* **2009**, *21*, 336.
(29) Lange, H.; Wötting, G.; Winter, G. *Angew. Chem.* **1991**, *103*, 1606; *Angew. Chem., Int. Ed.* **1991**, *30*, 1579.
(30) Schnick, W.; Huppertz, H.; Lauterbach, R. *J. Mater. Chem.* **1999**, *9*, 289.

according to the procedure mentioned above. The obtained single-source precursor powder was heated in a radio-frequency furnace according to the above procedure.

The identity of the product was verified by X-ray powder diffraction utilizing a STOE Stadi P powder diffractometer with Ge(111)-monochromatized Mo−$K_{\alpha 1}$ radiation ($\lambda = 0.7104$ Å). The X-ray diffraction pattern of doped $Sr_2Si_5N_8$ powder are in good agreement with the reported powder patterns in JCPDS 85−01. The powder patterns have also been double checked with patterns calculated from single crystal data.[19] The solid-solution $Ba_{1.5}Sr_{0.5}Si_5N_8$ was verified using Vegards rule[31] interpolating the crystal data of $Sr_2Si_5N_8$ and $Ba_2Si_5N_8$.[19]

Scanning electron microscopy was performed on a JEOL JSM-6500F equipped with a field emission gun at an acceleration voltage of 10 kV. Samples were prepared by placing the powder specimen on adhesive conductive pads and subsequently coating them with a thin conductive carbon film. Each EDX spectrum (Oxford Instruments) was recorded with the analyzed area limited on one single nanocrystal to avoid influence of possible contaminating phases.

FTIR measurements were carried out on a Bruker IFS 66v/S spectrometer. The preparation procedures were performed in a glovebox under dried argon atmosphere. Spectra were recorded at ambient conditions in the range between 400 and 4000 cm^{-1} by dispersing the samples in anhydrous KBr pellets.

Excitation and emission spectra were measured for powdered samples of the as-synthesized reaction product of $Sr_2Si_5N_8$:Eu and $Ba_{1.5}Sr_{0.5}Si_5N_8$:Eu^{2+} at Philips research laboratories, Aachen, by means of an in-house built spectrometer system equipped with a 150-W Xe arc lamp, a 2 × 500 mm Czerny Turner monochromator (1800 grooves/mm, 250/500 nm blaze gratings) and a SPC multiplier detection unit (modified FL900, Edinburgh Instruments, Great Britain).[32] For the calculation of CIE (Commission Internationale d'Eclairage) color coordinates (x, y) the emission spectra were weighted by the 10° standard observer CIE color matching functions. After summarizing, the obtained tristimulus values were normalized to obtain CIE 1933 color coordinates.

Thermoanalytical (TG/DTA) measurements were performed on a TGA 92−2400 (Setaram) thermoanalyzer equipped with gage heads. The samples were placed in an unsealed Al_2O_3 crucible and heated from RT to 700 °C with a rate of 5 °C min^{-1} (gas flow 100 mL min^{-1} helium 5.0).

Results and Discussion

Synthesis of Mixed-Metal Amide Precursor. The formation of metal amides by dissolving the respective metals (e. g. Ba, Sr, Eu) in liquid ammonia is well-known.[33] Recently, we have used these amides as precursors for the synthesis of 2-5-8-type nitridosilicate phosphor materials.[28] For the synthesis of defined solid solution compounds in the system $Sr_{2-x}Ba_xSi_2N_8$:Eu^{2+} thorough stoichiometry control has to be maintained throughout the synthesis. In classical solid-state processes the problem of relatively low interdiffusion coefficients of the binary nitrides is hampering this goal. However, the problem can easily be solved by application of a solution-based precursor process employing supercritical ammonia. The approach can be regarded as the ammonthermal counterpart of well known sol-gel processes because it ensures complete solution of the starting materials, followed by precipitation of the mixed product. The mixed amide precursor was synthesized with a molar ratio Ba/Sr/Eu of 1.5/0.5/1% at 150 °C and 300 bar. By dissolving the metals in supercritical ammonia complete mixing is achieved, lowering the diffusion paths significantly to the atomic level. Furthermore, a perfect distribution of europium is achieved by this approach, assuring a uniform doping of the resulting phosphor powder. The pure metal amides of strontium and barium are colorless, whereas europium amide has an orange color. The obtained precursors exhibit a pale yellow color, underlining the intimate distribution of $Eu(NH_2)_2$. The IR-spectrum of the obtained powder is depicted in Figure 1. The existence of several N−H stretching bands in the region of 3185−3265 cm^{-1} as well as N−H deformation bands ranging from 1509 to 1566 cm^{-1} prove the formation of metal amides.[34] The XRD pattern of the precursor (not displayed) revealed the formation of $Ba(NH_2)_2$ besides $Sr(NH_2)_2$. $Eu(NH_2)_2$ could not be detected in the XRD because the amount is too small. Strontium amide shows fluorescence under Mo-radiation, producing a noticeable background. EDX investigations confirmed the formation of a precursor with homogeneous distribution Ba/Sr/Eu in the solid.

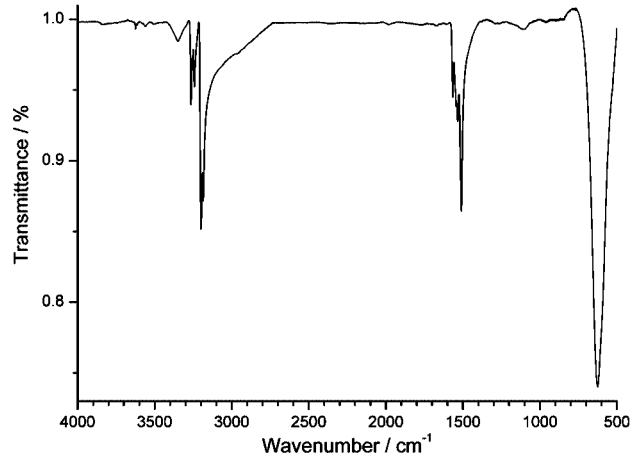

Figure 1. FTIR-spectrum (KBr pellet) of the mixed amide precursor [$Ba_{1.5}$/$Sr_{0.5}$/$Eu_{0.02}$]$(NH_2)_2$.

The thermal degradation of the Ba/Sr/Eu precursor was investigated by thermoanalytical measurements (DTA/TG). Four different thermal events can be identified as marked in figure 2. The endothermic peaks between 290 and 310 °C (1 and 2) can be attributed to the degradation of barium amide to barium imide.[35] Because the amount of europium within the sample is quite low, the endothermic peak of $Eu(NH_2)_2$ dissociation will probably be covered by the strong signals (1 and 2) of $Ba(NH_2)_2$. Around 440 °C (3), the onset of the decomposition of Sr amide to the respective imide is observed.[35] At higher temperatures around 590 °C (4), the endothermic signal indicates the starting reaction of the imides and formation of the respective nitrides. These in situ investigations gave a deeper insight into the complete conversion of the mixed metal precursor regarding the

(31) Vegard, L. *Z. Phys.* **1921**, *5*, 17.
(32) Jüstel, T.; Krupa, J.-C.; Wiechert, D. U. *J. Lumin.* **2001**, *93*, 179.
(33) Senker, J.; Jacobs, H.; Müller, M.; Press, W.; Müller, P.; Mayer, H. M.; Ibberson, R. M. *J. Phys. Chem. B* **1998**, *102*, 931.
(34) Linde, G.; Juza, R. *Z. Anorg. Allg. Chem.* **1974**, *409*, 199.
(35) Hartmann, H.; Fröhlich, H.; Ebert, F. *Z. Anorg. Allg. Chem.* **1934**, *218*, 181.

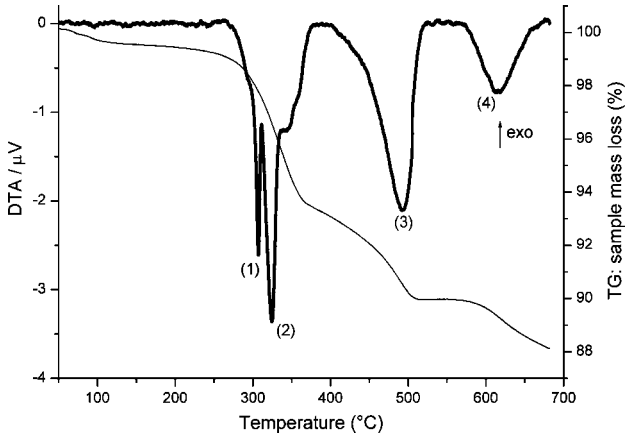

Figure 2. DTA (solid line) and TG (gray line) measurement of $[Ba_{1.5}/Sr_{0.5}/Eu_{0.02}](NH_2)_2$.

Table 1. Different Synthesis Conditions for $Ba_{1.5}Sr_{0.5}Si_5N_8:Eu^{2+}$

silicon source	phase	temperature (°C)	annealing time (h)	cooling time (h)
silicon diimide	Si-1	1300	24	12
silicon powder	Si-2	1400	12	12
nanocrystalline silicon	Si-3	1400	12	12

formation of reactive intermediates. Furthermore, at relatively low temperatures below 700 °C, the decomposition leads to in situ synthesized, reactive metal nitrides.

Reaction with Different Silicon Sources. The use of metals and silicon diimide in common synthetic approaches results in the formation of the respective metal nitrides and silicon nitride which react subsequently to the respective nitridosilicates. By applying the above mentioned reactive mixed-metal amide precursors, reaction with other silicon sources at comparably low synthesis temperatures is rendered possible. Because the amide precursor decomposes by releasing ammonia, elemental silicon may form an undefined silicon nitride imide or directly the silicon nitride at lower temperatures. In this context, the reaction behavior of the amide precursor with silicon diimide (Si-1), silicon powder (Si-2), and nanocrystalline silicon (Si-3) was studied. The reaction details are summarized in Table 1. The syntheses of the Ba/Sr 2-5-8 phases were performed at temperatures around 1300−1400 °C. These findings are in good agreement with recent investigations involving the reaction of silicon diimide and metal amides at low temperatures.[28] Furthermore, an extension to solid-solution materials exhibiting interesting luminescence properties was achieved. Usage of reactive metal amide precursor leads to the following benefits: The temperature can be lowered significantly without impairing luminescence efficiency.[28] Moreover, different silicon sources can be employed at quite low reaction temperatures because of the high reactivity of the amide precursor. A crucial point about varying the silicon sources is their influence on the crystal shape and the resulting luminescence properties of the products. Hence, the morphology and as a consequence the luminescence of the synthesized phosphor particles was compared with respect to different silicon sources (see below).

One-Pot Synthesis of Single-Source Precursors. Synthesis of 2-5-8 phosphor materials was further optimized by

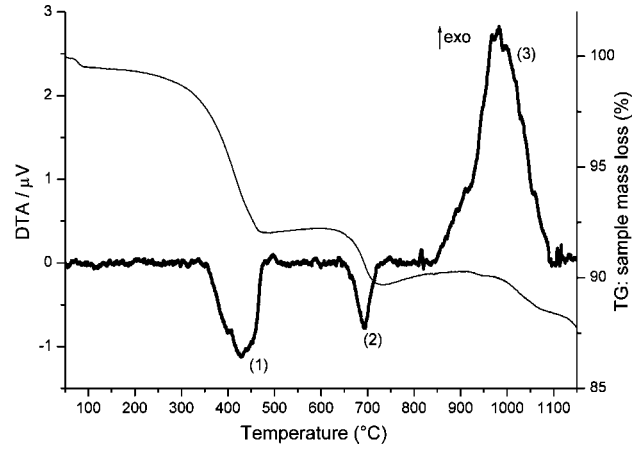

Figure 3. DTA (solid line) and TG (gray line) measurement of the single-source precursor ($Si_{nc}/Sr(NH_2)_2$).

Table 2. Synthesis Conditions for $Sr_2Si_5N_8:Eu^{2+}$ and $Ba_{1.5}Sr_{0.5}Si_5N_8:Eu^{2+}$ Starting from Single-Source Precursors

single-source precursor	phase	temperature (°C)	annealing time (h)	cooling time (h)
Sr/Eu/Si/N	Si-4	1400	12	12
Ba/Sr/Eu/Si/N	Si-5	1400	24	12

a simple one-pot process. Hence, the metals as well as nanocrystalline silicon (Si_{nc}) were directly placed inside the high-pressure vessel prior condensing ammonia on the starting materials. During the reaction, the metals are dissolved and a suspension of dispersed nanoparticles of silicon is generated. At the applied temperature (150 °C) and in absence of a mineralizer,[27] elemental silicon does not react with supercritical ammonia. Nevertheless, distribution of the Si-nanoparticles within the ammonia solution is intimate anyway. The approach was applied to a stoichiometric mixture of metallic Sr and Eu with Si_{nc} (precursor for Sr-2-5-8:Eu^{2+}) and a mixture of Ba/Sr/Eu metals with Si_{nc} (precursor for $Ba_{1.5}Sr_{0.5}Si_5N_8:Eu^{2+}$). In both cases, rather fluffy ocher powders were obtained. When exposed to air, these single-source precursors hydrolyze by releasing ammonia. Subsequently, the powder was placed into a tungsten crucible and heated in a radiofrequency furnace according to the temperature program given in table 2. For complete conversion, a low annealing temperature of 1400 °C was sufficient.

The reactivity of the single-source precursor ($Si_{nc}/Sr(NH_2)_2$) for synthesis of Sr-2-5-8 was investigated by in situ thermal measurements regarding the onset of the reaction (cf. Figure 3). The first endothermic process (1) beginning around 370 °C can be attributed to the onset of the first decomposition step of strontium amide forming the imide. The subsequent process (2) starting around 670 °C) can be assigned to the second decomposition step, forming the metal nitride. In conjunction with the degradation behavior of the metal amides mentioned above, mechanistic cognitions for the synthesis of nitridosilicates can be received. Hence, the broad exothermic signal around 920 °C (3) indicates the starting point of the reaction between silicon and strontium nitride. Because the used nanocrystalline silicon exhibits no signals in the DTA/TG itself, the onset of the reaction

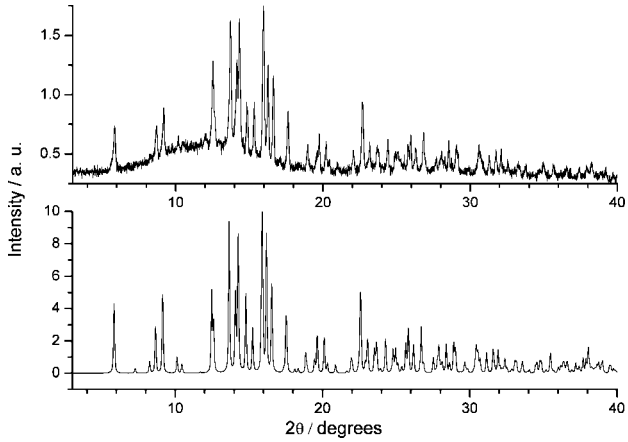

Figure 4. XRD pattern (Mo−$K_{\alpha1}$) of $Ba_{1.5}Sr_{0.5}Si_5N_8:Eu^{2+}$ (above) and simulated powder pattern of $Ba_2Si_5N_8$ (below).

between silicon and the metal amides regarding the formation of the 2-5-8 can be assigned to this temperature.

By applying this one-pot approach large amounts of defined single-source precursors for the 2-5-8 phosphors can be synthesized. Ammonothermal treatment of the starting materials at low temperatures (T = 150 °C) allows the use of Teflon-lined autoclaves and thus avoids contamination of the product by reaction with the container material. The XRD pattern of the as synthesized solid solution material $Ba_{1.5}Sr_{0.5}Si_5N_8:Eu^{2+}$ (Si-5) is depicted in Figure 4. The calculated pattern of $Ba_2Si_5N_8$ is displayed for comparison.[19] The XRD pattern was indexed using the software package STOE WinXPOW (Fa. Stoe & Cie GmbH, Darmstadt) revealing an orthorhombic system with lattice parameters of a = 934.9(3) pm, b = 692.1(2) pm, c = 575.3(1) pm, and $V = 372.2(1) \times 10^6$ pm^3 (40 reflections, FOM = 4.1). Sr-2-5-8 and Ba-2-5-8 crystallize isotypically in the orthorhombic space group $Pmn2_1$, but with slightly differing lattice constants.[19] In previous investigations, the molar ratio Ba/Sr was determined in solid solution studies according to the lattice parameters applying Vegards rule.[31,36] According to these investigations the formation of $Ba_{1.5}Sr_{0.5}Si_5N_8:Eu^{2+}$ can be confirmed on the basis of the indexed pattern mentioned above. The background in the powder pattern may be due to fluorescence of strontium under Mo radiation or traces of Ba/Sr orthosilicate, which could easily be removed by washing the product in diluted hot HCl. Nevertheless, EDX measurements confirmed the molar ratio Ba/Sr = 3/1 and indicate a molar ratio metal/Si = 1/2.5, corroborating the formation of the 2-5-8 phase.

Morphology. As already pointed out, morphology of the phosphor particles has a significant impact on the optical properties. Because of the rather high refractive index of the 2-5-8 phases (between 2 and 3)[37] and the anisotropical crystal morphology (high aspect ratio) total internal reflection of luminescence may be an issue for acicular particles. Because the one-pot approach fulfills all requirements like reactive metal precursors intimately mixed with silicon nanoparticles,

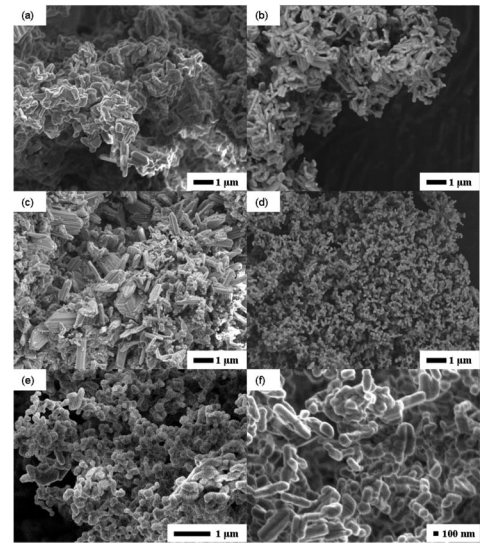

Figure 5. SEM images of (a, b) $Ba_{1.5}Sr_{0.5}Si_5N_8:Eu^{2+}$ after synthesis with silicon diimide (1300 °C); (c) $Ba_{1.5}Sr_{0.5}Si_5N_8:Eu^{2+}$ after synthesis with silicon powder (1400 °C); (d−f) $Ba_{1.5}Sr_{0.5}Si_5N_8:Eu^{2+}$ after synthesis with nanocrystalline silicon powder (1400 °C).

special attention was directed to the shape of the synthesized crystallites. In the following, the morphology of phosphor particles synthesized via mixing the pre-synthesized metal amides with silicon (mentioned above) and particles synthesized from single-source precursors obtained via one-pot approach were compared.

The influence of different silicon sources is depicted in Figure 5 by employing identical mixed amide precursor in each reaction. Quite low temperatures (1300 °C) are sufficient for complete reaction with silicon diimide (Si-1). The synthesized phosphor powder exhibits small agglomerated particles with uniformly shaped habit (figure 5 a, b). This observation corresponds to recent investigations regarding the reaction of single metal amides with silicon diimide and could now be extended to the employment of mixed metal precursors.[28] The reaction with microcrystalline silicon powder was performed at 1400 °C (Si-2, Figure 5c), corroborating the high reactivity of the applied precursor. The SEM image reveals barlike rods, with a clear tendency to crystalline material compared to the irregular particles of the reaction with silicon diimide, because of the larger silicon powder particles. The use of nanocrystalline silicon powder (Si-3) yields the formation of a uniform powder with small crystallites, visible in Figure 5d. A closer inspection revealed spherical phosphor particles (Figure 5e), in the range of 200 nm (Figure 5f). Because of the good distribution of the nanocrystalline silicon particles within the amide precursor, many small seeds are formed during the reaction, resulting in the formation of small particles with a narrow particle size distribution (PSD). This observation is quite interesting for phosphor powders, because it ensures constant luminescence properties due to uniformly shaped particles. Besides, silicon diimide turned out to be the most reactive silicon compound because the required temperature for complete reaction is about 100 °C lower compared to silicon powder and nanocrystalline silicon. However, the reactive amide precursor still allows the use of low temperatures (1400 °C)

(36) Stadler, F. Doctoral Thesis, University of Munich (LMU), Munich, Germany, 2006.
(37) Lutz, H.; Joosten, S.; Hoffmann, J.; Lehmeier, P.; Seilmeier, A.; Höppe, H. A.; Schnick, W. *J. Phys. Chem. Solids* **2004**, *65*, 1285.

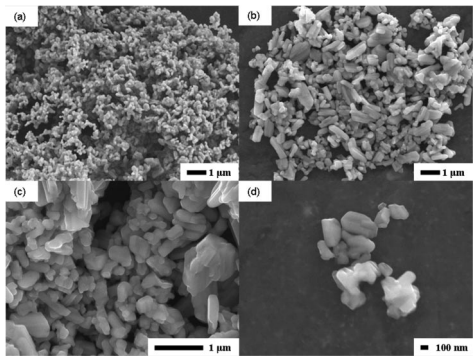

Figure 6. SEM images of (a) $Sr_2Si_5N_8:Eu^{2+}$ synthesized from single-source precursor (1400 °C); (b−d) solid-solution $Ba_{1.5}Sr_{0.5}Si_5N_8:Eu^{2+}$ synthesized from single-source precursor (1400 °C).

in combination with relatively "unreactive" silicon sources like silicon powder or Si_{nc}.

Special attention was directed to the morphology of the obtained 2-5-8 phases starting from pre-synthesized single-source precursors (with Si_{nc}) obtained via one-pot synthesis (Si-4; Si-5; Table 2). The resulting powders are examined as synthesized, without post annealing or washing of the product (figure 6). The $Sr_2Si_5N_8:Eu^{2+}$ phase consists of uniformly shaped globular particles with smooth edges and without vertices, exhibiting a size of ∼200 nm forming nanocrystalline phosphor material (cf. Figure 6a; Si-4). The solid solution material $Ba_{1.5}Sr_{0.5}Si_5N_8:Eu^{2+}$ revealed a slightly broader distribution of particle shapes. Besides the known spherical crystallites, some bar-like particles can be detected (Figure 6b; Si-5). However, these "larger" crystallites exhibit sizes of ∼1 μm and a tendency to smooth edges can be observed. The formation of barlike particles can presumably be attributed to the high amount of barium within the product. Recent investigations on the formation of Ba 2-5-8 phases revealed an analogous tendency, not observed for the Sr 2-5-8 phase.[28] Nevertheless, EDX measurements of different particles proved the presence of both Ba and Sr within the single crystals independent from their size. A closer inspection of the crystals (Figure 6c) reveals coalescent particles; however, single crystals with particle size between 150 and 200 nm can be distinguished (Figure 6d). This tendency can be vaguely discerned for Sr 2-5-8 but occurs previously for the solid solution material. Because of the application of the single-source precursor approach a similar distribution of the silicon nanoparticles is ensured. Therefore, the slightly different reaction behavior of the solid solution 2-5-8 phase compared to Sr 2-5-8 is responsible for different particle morphology.

Luminescence. The optical properties of phosphor samples ($Ba_{1.5}Sr_{0.5}Si_5N_8:Eu^{2+}$) synthesized by reaction of the mixed metal amide precursor with silicon diimide (Si-1) and nanocrystalline silicon (Si-3) were determined and compared with those synthesized by standard methods. The emission spectra of the two synthesized powders are displayed in Figure 7. According to Table 1, the reaction with silicon diimide was performed at 100 °C lower compared to the synthesis with nanocrystalline silicon. But longer reaction times have proven to counteract low temperatures in the case of luminescence properties.[28] In both cases, the measurements were carried out at RT with excitation at 450 nm due to the

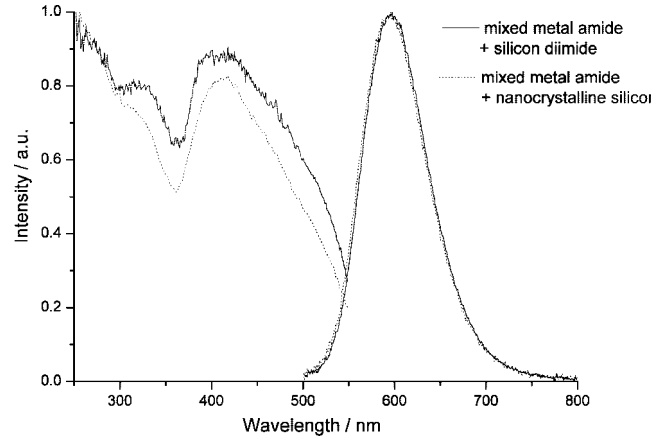

Figure 7. Photoluminescence spectra of ($Ba_{1.5}Sr_{0.5}Si_5N_8:Eu^{2+}$); reaction product of the mixed metal amide precursor with silicon diimide (Si-1) and nanocrystalline silicon (Si-3) (λ_{exc} = 450 nm).

Table 3. Optical Properties of the Synthesized $Ba_{1.5}Sr_{0.5}Si_5N_8:Eu^{2+}$ and $Sr_2Si_5N_8:Eu^{2+}$ Phosphors

phase	$\lambda_{emission}$ (nm)	CIE color coordinates x	CIE color coordinates y	lumen equivalent (lm/W)	rel. quantum efficiency (%)
Si-1	597	0.562	0.435	373.1	99
Si-3	595	0.555	0.442	385.9	95
Si-4	609	0.619	0.380	266.5	80
Si-5	592	0.543	0.452	421.3	77
reference sample[28]	625	0.634	0.365	215.0	100

well-known strong absorption of the 2-5-8 phases in the range of 380−500 nm.[2,11] Hence, these phosphors may efficiently be excited by (In,Ga)N LEDs. The emission spectra revealed two very similar curves, with maxima at 597 and 595 nm for reaction with Si-1 and Si-3, respectively. The high reactivity of the mixed metal amide precursor and the perfect distribution, resulting in identical molar ratios of the starting materials can be considered as constant for both materials. Hence, the variation of silicon sources has only small influence on the emission wavelength whose maxima differ less than 0.35 %. The full width at half maximum (FWHM) of both phosphors is identical within experimental errors (84.1 nm for Si-1 and 83.5 nm for Si-3). Table 3 presents the optical parameters for Si-1, Si-3, and a reference sample synthesized by standard methods ($Sr_2Si_5N_8:Eu^{2+}$, 1550 °C).[28] The quantum efficiency of Si-1 is comparable to the reference value, while sample Si-3 is slightly less efficient. These results corroborate the applicability of this novel precursor approach for the synthesis of LED phosphor materials. In addition to excellent luminescence properties, a very homogeneous distribution of the dopant is ensured. Furthermore the use of nanocrystalline silicon results in uniformly shaped phosphor particles without decreasing efficiency and simultaneously reducing synthesis efforts. $Sr_2Si_5N_8:Eu^{2+}$ synthesized from single-source precursor exhibit good optical parameters (cf. Table 3; Si-4) in combination with nanocrystalline phosphor particles (Figure 6a). These findings can be corroborated by the optical properties of the nanocrystalline solid solution phosphor $Ba_{1.5}Sr_{0.5}Si_5N_8:Eu^{2+}$ synthesized via the single-source precursor yielded in the one-pot reaction of the respective metals (cf. Table 3; Si-5). The lower quantum efficiency of Si-5 can be explained by small

amounts of Ba/Sr orthosilicates mentioned above, which could be removed by washing in diluted hot HCl. Furthermore, to compare optical properties with the particle size, no post annealing was performed, which would be an easy way to remove defects and further increase the optical properties.

Conclusion

The nitridosilicate phosphors $M_2Si_5N_8:Eu^{2+}$ with M = Sr, Ba for white light emitting diodes have been successfully synthesized using a novel one-pot approach to single-source precursors for these phosphor materials. By reacting the starting materials in supercritical ammonia, complete reaction and mixing at the atomic level is ensured. The reaction behavior of different silicon sources with the mixed metal amides was investigated, corroborating the high reactivity of the amides and revealed major influence on the crystal shape. The use of microcrystalline silicon powder yielded more coarsely crystalline particles with sharp edges, whereas reaction with nanocrystalline silicon results in the formation of spherical phosphor nanoparticles. The influence of different silicon sources on the optical properties revealed only small differences in emission maximum or lumen equivalent. Therefore, tailormade morphology control can be achieved, without impairing the luminescence properties. Furthermore, the in situ reactivity of the single-source precursor for $Sr_2Si_5N_8:Eu^{2+}$ revealed the onset of the formation of the phosphor material at rather low temperatures around 920 °C. Additionally, this approach yielded similar luminescence properties as compared to conventionally synthesized phosphor powders. In conjunction with rather low synthesis temperatures of 1300−1400 °C, this precursor approach is quite promising for further industrial and scientific applications and presumably can be successfully applied to the synthesis of other nitridosilicates.

Acknowledgment. We thank H. Höller for conducting the DTA/TG measurements as well as C. Minke for performing the SEM and EDX measurements (both LMU Munich; Department Chemie und Biochemie). The authors gratefully acknowledge financial support by the Fonds der Chemischen Industrie (FCI).

CM900341F